

浅間山浅部の比抵抗構造とマグマの移動

Shallow Resistivity Structure of Asama Volcano and its Implications for Magma Ascent Process in the 2004 Eruption

浅間火山電磁気構造探査グループ・相澤広記(東工大・火山流体)

Koki Aizawa, Yasuo Ogawa, Takeshi Hashimoto, Takao Koyama, Wataru Kanda, Yusuke Yamaya, Masaaki Mishina, Tsuneomi Kagiya, E. Koyama, H. Tsuji, A. Okubo, A. Suzuki, J. Hirabayashi, K. Nogami, S. Uto, S. Nagaoka, K. Saho, and Y. Tanaka

Resistivity Structures

Asama volcano is an active volcano with many historical records of Vulcanian eruptions. Its most recent eruptions occurred in 2004 at the summit crater. In this study, we argue the resistivity structure shallower than 3 km obtained by a dense magnetotelluric survey. The magnetotelluric data were obtained at 74 measurement sites mainly along the four survey lines across the volcano (**Fig. 1**). The resistivity profiles obtained by two-dimensional inversions (**Fig. 2 and 3**) are characterized by a resistive surface layer and an underlying conductive layer. The dominant feature of the profiles is the existence of three resistive bodies (marked by broken lines) at a depth range of a few hundred meters to a few kilometers surrounded by a highly conductive region. Considering that two of the three resistive bodies correspond to the old eruption centers (one corresponds to the 24 ka collapse caldera and the other to the 21 ka lava dome), the resistive bodies imply zones of old and solidified intrusive magma with low porosity. Because geothermal activities exist near the resistive bodies, the enclosing highly conductive regions are interpreted as a hydrothermal system driven by the heat from the old solidified magma.

Model for magma movement in the 2004 eruptions

In Asama volcano, the continuous GPS data suggested magma (dike) intrusion at a depth of 3 km around the west of the present active crater, though the confidence limits are several km (Aoki et al., 2005; Murakami, 2005). The estimated dike orientation is approximately E-W in both models and is consistent with the direction of the regional compression stress field around Asama volcano (Seno, 1999). The E-W direction is also consistent with the evolution history of Asama volcano. **Figure 4** schematically shows the recent magma intrusive zone with possible location errors and three old solidified magma of high resistivity. The magma intrusive zone is geodetically determined approximately beneath the swarm of VT earthquakes located at the bottom of the resistive body under the 24 ka collapse caldera. This evidence suggests structural control on magma movement in the 2004 eruptions.

As shown in **Fig. 4**, we propose the following scenario for the magma ascent process in the 2004 eruptions. Magma from the lower crust first ascended toward the 24 ka collapse caldera. Then, the magma ascent was impeded by the old solidified magma (resistive body) at a depth around 3 km, resulting in magma accumulation and subsequent pressure increase that probably triggered the VT earthquake. After the emplacement of magma at a depth deeper than 3 km, part of the magma migrated horizontally to the east and finally ascended to the summit, resulting in the 2004 eruptions.

Since the GPS analysis of another period (1997–2005) suggested that the recent intrusive zone in Asama is stable (Murakami, 2005), and remarkable earthquakes are not detected deeper than 3 km, the pathway from the deeper part to the 3 km depth may be a long-term persistent magma plumbing system that uses the established conduit. The old large stratovolcano (Kurofu volcano) may have also used this conduit before its edifice collapse. The possible deep magma ascent route is clearly revealed by the deep MT sounding (Ogawa et al., 2006).

There are three possibilities that explain the structural control by old solidified magma on the present magma movement. The first possibility is the density of solidified magma. If the density of ascending melt is balanced to that of solidified magma, the ascent may stop there; that is, old solidified magma acts as a density barrier for ascending magma. The second possibility is that solidified magma is hard to fail, or alternatively ductile. Because ascending magma cannot generate a crack in the solidified magma, it seeks another ascending route. The third is the stress field caused by old magma intrusion. If an old intrusive magma induces a great compressive stress field around it, the subsequent ascending magma cannot intrude

near the old intrusion. The study of the precise hypocenter location east of Izu Peninsula, Japan, suggested that the propagation direction of a dike is governed by the stress field caused by the previous dike intrusion (Hayashi and Morita, 2003). Such a situation is also experimentally replicated by Takada (1994) using gelatin cracks. Future precise gravity and active seismic surveys would constrain the physical property of the resistive bodies and grade the significance of the possibilities proposed.

Conclusion

This study raises the possibility that solidified remnant magma in the top few kilometers within volcanoes is controlling the present magma movement. Old remnant magma should be one of the key targets to study the relationship between magma movement and structure. The detection of old magma in the shallow part of volcanoes may contribute to an understanding of the present magma plumbing system and also volcano history.

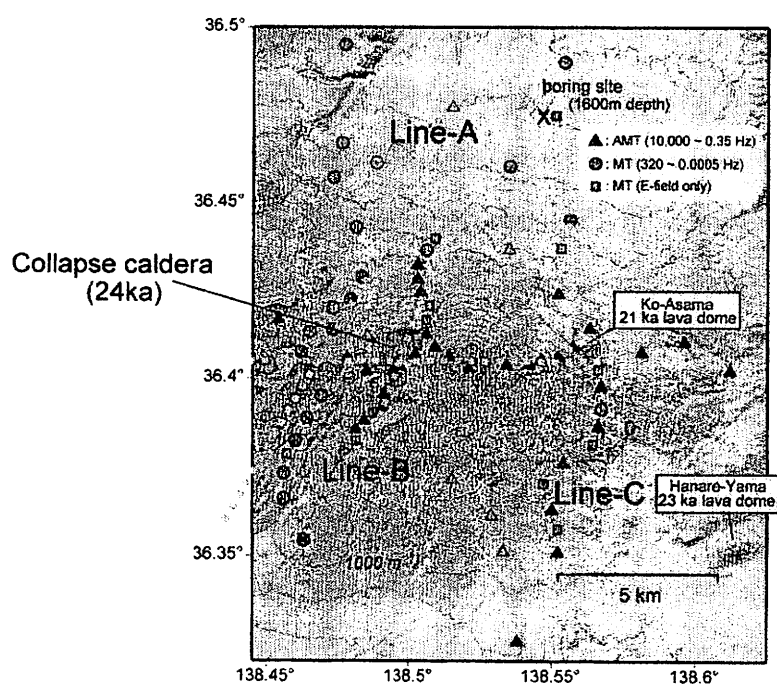


Fig. 1. 2-D magnetotelluric survey lines. Measurement sites used in 2-D inversions are shown as solid symbols. The triangles and circles show the AMT (10000–0.3 Hz) and MT (300–0.0005 Hz) sites, where both electric and geomagnetic fields were measured. Squares indicate MT sites at which only the electric field was measured. Red patches represent surface geothermal manifestation. Major topographic features are noted in the figures. The topographic contour interval is 100 m. The westernmost survey line (Line-A) is reported by Ogawa et al. (2006). There are three approximate N-S survey lines and one E-W survey line.

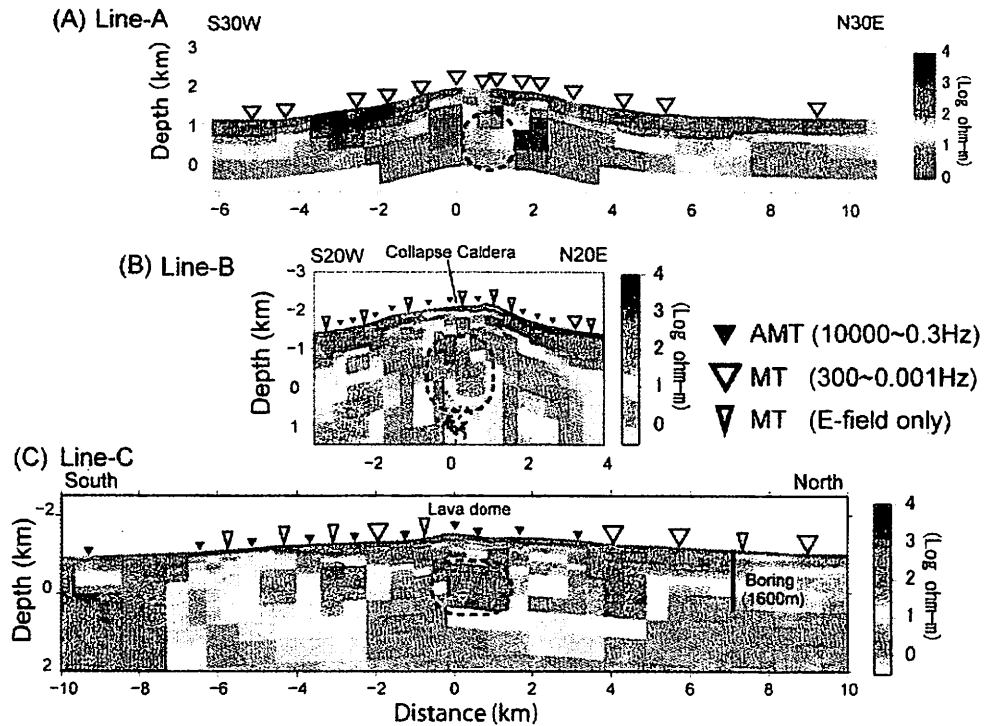


Fig. 2. The best-fit resistivity models of approximate N-S survey lines. The models were obtained by 2-D inversion using the code of Ogawa and Uchida (1996). All impedances were decomposed using site-dependent and frequency-independent distortion parameters (Groom and Bailey, 1989); then, we inverted the decomposed apparent resistivity, the phase, and the projected geomagnetic transfer function. Three resistivity profiles are shown from the west (upper) to the east (lower). (A) represents the shallow resistivity structure taken from Ogawa et al. (2006). Survey lines and locations of the measurement sites are shown in Fig. 1. The inverted triangles indicate the measurement sites. In the profile of survey Line-B (B), volcano-tectonic (VT) earthquakes (Takeo et al., 2006) are also shown. Note that the seismicity around other profiles is low. The resistive bodies discussed in the text are marked as broken lines.

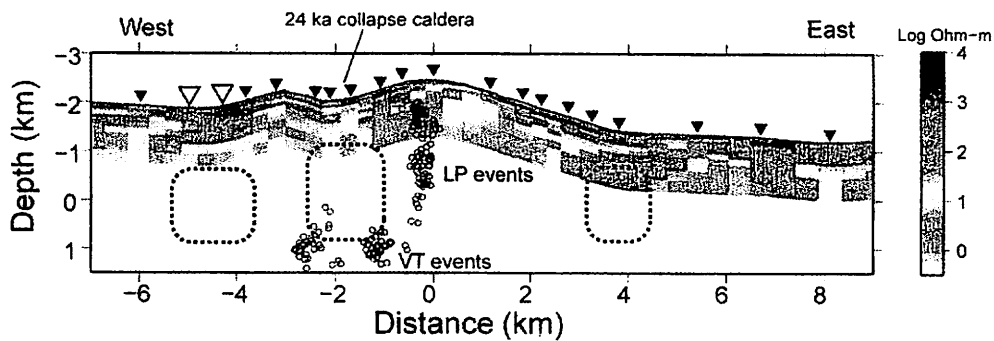


Fig. 3. The best-fit resistivity models of E-W survey line. The models were obtained by 2-D inversion mainly using AMT data. Survey lines and measurement sites are shown in Fig. 1. The decomposed TM and TE mode data and geomagnetic transfer functions were used for the inversion. Data in the frequency lower than 10 Hz were not used because of the conflict with the estimated 2-D strike. The inverted triangles indicate the measurement sites. The locations of resistive bodies, which were imaged by the analysis of N-S profiles (Fig. 2), are marked as broken lines. Volcano-tectonic (VT) and low frequency (LP event) earthquakes, which occurred from January 2004 to October 2005 (Takeo et al., 2006), are also shown.

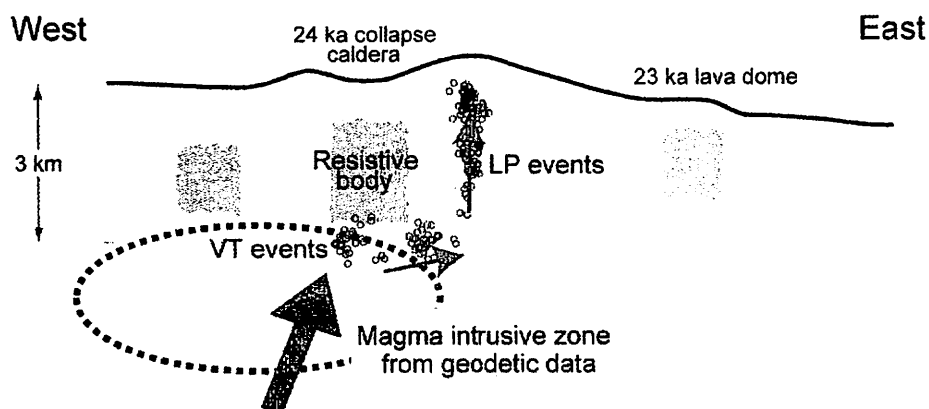


Fig. 4. A schematic model of magma ascent process in the 2004 eruptions. Gray patches represent the resistive bodies imaged in this study. Hypocenters of volcano-tectonic (VT) and low-frequency (LP event) earthquakes (Takeo et al., 2006) are also shown. Inferred magma movement is represented by solid arrows. Possible magma intrusive zone determined by geodetic data (Aoki et al., 2005; Murakami, 2005) are shown as a broken ellipse. Note that these geodetic models are not well constrained in terms of the location (error is approximately several km).

Acknowledgments

H. Tsuji monitored the volcanic activity at the observatory and contributed to the safe conduct of the field surveys. Esashi Geomagnetic Observatory, Geographical Survey Institute, provided the geomagnetic data for remote reference processing in this study. The hypocenter data was provided by M. Takeo. This study was supported by the 7th national project for the volcano eruption prediction. One of the authors, K. Aizawa, is now supported by JSPS research fellowship.

References

- Aoki Y., Watanabe, H., Koyama, E., Oikawa, J., Morita, Y., 2005. Ground deformation associated with the 2004-2005 unrest of Asama volcano, Japan. *Kazan*, 50, 575-584. (in Japanese with English abstract)
- Hayashi, Y., Morita, Y., 2003. An image of a magma intrusion process inferred from precise hypocentral migrations of the earthquake swarm east of the Izu Peninsula. *Geophys. J. Int.*, 153, 159-174.
- Ogawa, Y., Uchida T., 1996. A two-dimensional magnetotelluric inversion assuming Gaussian static shift, *Geophys. J. Int.*, 126, 69-76.
- Ogawa, Y., Aizawa, K., Hashimoto, T., Koyama, T., Electromagnetic Research Group for Asama volcano, 2006. Magnetotelluric observation across the dyke intrusion of Asama volcano. 18th Electromagnetic Induction Workshop, El Vendrell, Spain, September 17-23.
- Seno, T., 1999. Syntheses of the regional stress fields of the Japanese islands. *Island Arc*, 8 (1), 66-79, doi:10.1046/j.1440-1738.1999.00225.x.
- Takada, A., 1994. Development of a subvolcanic structure by the interaction of liquid-filled cracks. *J. Volcanol. Geotherm. Res.*, 61, Issues 3-4, 207-224.
- Takeo, M., Aoki, Y., Ohminato, T., Yamamoto, M., 2006. Magma supply path beneath Mt. Asama volcano, Japan. *Geophys. Res. Lett.*, 33, L15310, doi:10.1029/2006GL026247.
- Murakami, M., 2005. Magma plumbing system of the Asama volcano inferred from continuous measurements of GPS. *Kazan*, 50, 347-361. (in Japanese with English abstract)